1

2

3   **Wave attenuation over coastal salt marshes under storm surge conditions**

4   **Authors:**

5   **Iris Möller**[1,2] *****

6   **Matthias Kudella**[3]

7   **Franziska Rupprecht**[4]

8   **Tom Spencer**[1]

9   **Maike Paul**[3]

10   **Bregje K. van Wesenbeeck**[5]

11   **Guido Wolters**[5]

12   **Kai Jensen**[4]

13   **Tjeerd J. Bouma**[6]

14   **Martin Miranda-Lange**[3]

15   **Stefan Schimmels**[3]

16

17   *** corresponding author**

---

[1] Cambridge Coastal Research Unit, Department of Geography, University of Cambridge, Downing Place, Cambridge, CB2 3EN, UK; email: im10003@cam.ac.uk.
[2] Fitzwilliam College, Storey's Way, Cambridge CB3 0DG, UK.
[3] Forschungszentrum Küste (FZK), Merkurstr. 11, 30419 Hannover, Germany.
[4] Applied Plant Ecology, Biocenter Klein Flottbek, University of Hamburg, Ohnhorststr. 18, 22609 Hamburg, Germany.
[5] Deltares, Rotterdamseweg 185, 2629 HD Delft, NL.
[6] Yerseke Spatial Ecology, Netherlands Institute for Sea Research (NIOZ), Korringaweg 7, 4401 NT Yerseke, NL.

18

Coastal communities around the world face increasing risk from flooding as a result of rising sea level, increasing storminess, and land subsidence[1–2]. Salt marshes can act as natural buffer zones, providing protection from waves during storms[3–7]. However, the effectiveness of marshes in protecting the coastline during extreme events when water levels are at a maximum and waves are highest is poorly understood[8,9]. Here, we experimentally assess wave dissipation under storm surge conditions in a 300-meter-long wave flume tank that contains a transplanted section of natural salt marsh. We find that the presence of marsh vegetation causes considerable wave attenuation, even when water levels and waves are highest. From a comparison with experiments without vegetation, we estimate that up to 60% of observed wave reduction is attributed to vegetation. We also find that although waves progressively flatten and break vegetation stems and thereby reduce dissipation, the marsh substrate remained stable and resistant to surface erosion under all conditions. The effectiveness of storm wave dissipation and the resilience of tidal marshes even at extreme conditions suggests that salt marsh ecosystems can be a valuable component of coastal protection schemes.

Coastal margins are experiencing increased pressure from both physical environmental (sea level rise, increased storminess[10]) and human use (increased population densities, resource requirements[11]) perspectives. This has resulted in a re-evaluation of coastal flood and erosion risk reduction methods[5]. Natural coastal landforms, including sand dunes, mudflats and salt marshes, are now widely recognised as potential barriers to wave and tidal flow or as wave/tidal energy buffers[7,11–13]. The inclusion of such natural features into quantitative flood risk assessments, however, has been hampered by a lack of (i) empirical evidence for their capacity to act as wave dissipaters under extreme water level and wave conditions (when their coastal protection service is most required); and (ii) a quantitative understanding of their ability to survive those types of conditions[8,14–16].

43   Previous studies have suggested that wave dissipation over submerged salt marsh canopies is

44   dependent on water depth and incident wave energy, and that hydrodynamic conditions may exist

45   beyond which marshes lose their wave dissipating effect[6,17,18]. The existence of such conditions

46   makes intuitive sense, as the orbital wave motion that is affected by the submerged vegetation

47   canopy decreases with increasing depth and decreasing incident wave energy. Existing empirical

48   studies of wave reduction over vegetated canopies have, however, been limited to low water depths

49   (< 1 m) and low wave heights (< 0.3 m)[18,19].

50   Salt marsh resistance to wave impact is intricately connected to wave dissipation over salt marsh

51   surfaces[20]. Under high energy conditions, dissipation of wave energy may be achieved by wave

52   shoaling/breaking as well as removal of material (both plant and soil) from the marsh edge/surface,

53   rather than only by drag from the vegetation canopy[19]. Existing evidence points to the stabilising

54   effect of organic matter with respect to resistance of the marsh surface to erosion by waves from

55   above (with contrasting evidence for roots increasing erosion on exposed marsh margins)[21]. Little is

56   known, however, about the response of the marsh soil to extreme levels of wave impact, as might

57   be experienced during a storm surge. The stability of the marsh surface under such conditions is

58   critical to any assessment of its usefulness as part of coastal flood risk reduction schemes.

59   Here we present results of a unique large scale flume experiment with three key aims: to explore the

60   dissipation of waves over a vegetated marsh canopy under storm conditions; to quantify the effect

61   of vegetation on wave attenuation compared to the effects of a mowed platform; and to quantify

62   the response of marsh vegetation and soil surface to incident wave energy.

63   Waves were generated in a 300-m-long, 5-m-wide, and 7-m-deep flume over a test section of almost

64   40m length consisting of a coherent patchwork of marsh blocks (Fig. 1a). Blocks were characterized

65   by a mixed canopy of *Elymus athericus, Puccinellia maritima,* and *Atriplex prostrata*, typical of mid to

66   high southern North Sea marsh communities (Fig. 1d). Whereas incident wave heights on salt marsh

67   margins are limited by shallow inshore water depths and thus are generally low (<0.3 m), above-

68   marsh water depths are known to reach or exceed 2 m, accompanied by wave heights (H_s) in excess

69   of 0.8 m, during storms[19]. Tests were thus conducted for regular and irregular non-breaking waves of

70   heights up to 0.9m in 2m water depth above the vegetated bed. There was no statistical difference

71   between flume and field soil bulk density, stem diameter, and plant stem flexibility (Young's

72   Modulus) (t-test; p>0.05) (see Table 1 and Supplementary Information for detail).

73   Results show a clear dissipation pattern, remarkably consistent between regular and irregular waves.

74   For regular waves, wave energy dissipation over the 40m distance increased linearly from no

75   dissipation in the case of waves with H=0.1m and T=1.5s to 19.5% reduction for H=0.3m and T=3.6s

76   (Fig. 2a). For irregular waves, dissipation between 11.9 and 17.9% occurred for $H_{rms,0}$ of 0.2-0.4m

77   (Fig. 2b). When incident wave heights increased beyond these levels, dissipation reduced to 13.8%

78   for regular (H=0.6m, T=3.6s, Fig. 2a) and to 14.7% for irregular waves ($H_{rms,0}$=0.6m, T_p =4.0s, Fig. 2b),

79   before increasing to 16.9% for the largest regular waves (H=0.7 and 0.9m; T=5.1 and 4.1s) and to

80   16.9% for the largest irregular waves ($H_{rms,0}$ =0.7m, T_p=6.2 s).

81   Dissipation over the mowed surface was significantly lower in all regular wave tests (t-test, p<0.05)

82   (Fig. 2a) and irregular wave tests (Figure 2b). At (or just after) the point of maximum wave

83   dissipation (H and $H_{rms,0}$ = 0.2-0.4 m), wave height reduction over the mowed section was lower than

84   over the section with intact vegetation by a factor of 0.4. Thus it can be stated that the vegetation

85   cover alone accounted for 60 % of wave height reduction (Fig. 2a,b). However, when $H_{rms,0}$ increased

86   towards 0.6m, the vegetation cover accounted for only 40% of wave height dissipation (Fig. 2b).

87   Models of wave dissipation by vegetated beds commonly rely on knowledge of the drag coefficient

88   C_D incorporated into a friction factor that takes account of vegetation stem density, height, and

89   diameter. The complex nature of salt marsh vegetation precludes the *a priori* determination of C_D

90   from simple plant metrics. Nevertheless, an exponential decay relationship between the stem

91   Reynolds number Re_V and C_D of the form $C_D = a+(b/Re_V)^c$ has been found to exist for other vegetation

92   types[22-24]. Here, Re_V is a function of wave orbital velocity and the vegetation stem diameter. We

93   initially used our vegetation metrics (Table 1) and the C_D-Re_V relationship developed for seagrasses

94   to predict dissipation for our experimental conditions[22]. Figure 2a, b clearly shows that our observed

95   dissipation exceeded that predicted by a factor of 1.5-2.2 for regular and 2.6-3.2 for irregular waves.

96   We then calculated C_D for each experimental run from observed dissipation and plant metrics. C_D

97   decreased with increasing Reynolds numbers Re_V, confirming the established exponential

98   relationship between Re_V and C_D ($r^2 \geq 0.97$), but with coefficients a, b, and c that differ from those of

99   previous studies (see Supplementary Information).

100   Analysis of video footage showed that the reduction in dissipation for regular waves exceeding 0.3m

101   in height was accompanied by a change in behaviour of the marsh vegetation. Under relatively low

102   incident waves (H<0.3m; T<3.6s), the plants swayed and interacted with wave motion throughout

103   the wave cycle (Figs. 2a and 3a). For larger waves (stronger currents), however, stems bent over to

104   angles>50° during the forward wave motion, allowing the flow for part of the wave cycle to skim

105   over, rather than travel through the vegetation, thus retaining energy and reducing dissipation (Figs.

106   2a and 3b).

107   Video observations confirmed that this flattening of the plants preceded the tendency for plant

108   stems to fracture along lines of weakness that formed when stems folded over to high bending

109   angles. Cumulatively, this breakage resulted in a loss of 31% (30 kg) of the total 98 kg of biomass

110   after two days of runs under higher energy conditions (Fig. 2c). Such loss of plant material may then

111   have contributed to the reduced dissipation (Fig. 2a, b). The soil surface remained remarkably stable,

112   with an average lowering that was not significantly different from zero (4.4±10.4mm over the entire

113   experiment). The trend for average surface lowering from one surface exposure to the next was

114   greatest during the test runs with the largest waves, rather than during the test runs that resulted in

115   the largest release of plant biomass (Fig. 2c).

116   Wave attenuation of > 80 % has been reported in the literature for distances of about 160m under

117   low energy conditions[19]. The spatially non-linear nature of wave dissipation means that a conversion

118 of this figure to units of per cent per metre makes little sense[4], but the evidence presented here

119 shows that non-breaking wave dissipation can still reach 20% over a 40m distance even in water

120 depths typically found during storm conditions. This contribution is generated not only by the marsh

121 platform but also, and significantly, by the vegetation canopy. Moreover, we identify process

122 transitions in wave dissipation across the submerged salt marsh surface, associated with specific

123 incident wave energy levels. The spatio-temporal non-linearity in wave dissipation over coastal

124 wetlands has been linked to, amongst other factors, variability in the characteristics of the

125 vegetation cover (for example, flexibility[25]).The established general nature of the relationship

126 between Re_V and C_D seems robust, even for storm conditions, but the coefficients describing this

127 relationship in our experiment differ markedly from those established for lower energy conditions

128 and different vegetation types[22-24]. For regular waves of around 0.6m height (Re_V of around 640),

129 however, the model based on the empirical Re_V-C_D relationship leads to an over-prediction of

130 dissipation (see Fig. 2a) that warrants further investigation. We thus call for a re-evaluation of

131 existing wave dissipation models and urge the scientific community to develop more appropriate

132 methods for the *a priori* quantification of vegetation-induced drag for a broader range of plant

133 species and wave conditions. Ideally, such methods should be able to quantify drag directly from

134 plant metrics and knowledge of the incident flow field. Furthermore, the high bending angle and

135 repeated bending of vegetation under energetic conditions lead to plant breakage along lines of

136 weakness and a loss of biomass, a process that needs to be adequately represented in models of

137 marsh canopy growth/recovery after storm incidence.

138 The higher than expected rates of storm wave dissipation and the fact that marsh surfaces are able

139 to withstand larger wave forces without substantial erosion effects increase their reliability as part

140 of coastal defence schemes and shifts debates about marsh stability and resilience to those locations

141 where the marsh profile is exposed. In such settings, lateral retreat (for example cliff

142 undercutting/collapse on marsh fronts and channel widening)[26-28] may be enhanced by the presence

143 of vegetation, for example when roots become exposed to wave impact[21]. The long-term balance

144 between vertical and lateral marsh dynamics thus becomes a key area for further study[8,9].

145 The evidence presented here can serve as a validation data set for a new and improved

146 representation of drag and friction effects in numerical models of wave dissipation and vegetation

147 movement under storm conditions. It also supports the incorporation of salt marshes into coastal

148 protection schemes, such as the Dutch 'building with nature' approach[5,11,20]. Any such schemes must

149 carefully consider incident wave heights and water depths, alongside wave dissipation requirements

150 and the ecological conditions necessary for the maintenance of a healthy vegetation canopy.

151 **METHODS**

152 **Experimental set-up.** Experiments were conducted in the Large Wave Flume (Grosser Wellenkanal,

153 GWK) of Forschungszentrum Küste (FZK) in Hannover, Germany. The flume is the largest freely

154 accessible wave tank in the world; it is 310m long, 5m wide and 7m deep. The vegetated test section

155 of 39.44m length (about 180m^2) consisted of vegetated marsh blocks of 1.2m length, 0.8m width,

156 and 0.3m depth, cut from a natural marsh on the mainland coast in Eastern Frisia, German Wadden

157 Sea. The vegetated section was positioned on a 1.2m high sand base covered in geotextile at a

158 distance of 108m from the wave paddle and illuminated to prevent plant deterioration when

159 exposed. Adjacent to the front and rear end of the vegetated test section, a flat concrete surface

160 and ramped concrete slope allowed waves to shoal (Fig. 1a).

161 **Wave conditions and inundation schedule**. The flume was filled with fresh water to 2.0m water

162 depth above the vegetated soil surface and seven wave heights (H_{m0}: 0.1, 0.2, 0.3, 0.4, 0.6, 0.7 and

163 0.9 m) were simulated. Irregular waves (N ≥ 1000) were generated using a JONSWAP spectrum with

164 a peak enhancement factor of 3.3, followed by a regular wave run (N ≥ 100). After each two days of

165 tests, the flume was drained and exposed for at least 12h to allow plants to acquire oxygen. Tests

166   were conducted with initially intact and then mowed vegetation to determine the effect of the

167   vegetation as opposed to the topographic effect of the soil base.

168   **Wave measurements.** Sixteen wire wave gauges were deployed in sets of four (to enable reflection

169   analysis at each location). Here we report analysed wave parameters from sets 2 and 4 that relate to

170   the changes in wave characteristics over the full 40m of the vegetated section (see Fig. 1a,d). Wave

171   gauges within each set were separated in the direction of wave travel by 2.07m (front two gauges),

172   1.55m (middle two), and 1.58m (back two).

173   **Wave analysis.** For the regular wave tests, the first 11 fully developed waves were found to be

174   entirely unaffected by reflection from the flume end and were used to determine average wave

175   height (H, from min-max water surface elevations) and period (T, from zero-upcrossing points). For

176   irregular wave tests, the root-mean-square wave height in front of ($H_{rms,0}$) and behind ($H_{rms,1}$) the

177   vegetated section was calculated after reflection analysis, as described in the Supplementary

178   Information. Dissipation was analysed by comparing values at the last gauge of set 2 (3.02m in front

179   of the vegetated section) and the first of set 4 (2.2m behind the vegetated section) and expressed as

180   positive percentage of the wave height at the start of the section. If present, error bars indicate the

181   standard deviation of the difference between the wave heights.

182   **Wave dissipation model.** Dalrymple et al.'s[29] model was used to compute the dissipation of regular

183   waves and Mendez and Losadas'[30] model was applied to irregular waves over the 40 m long

184   vegetated section x with H_0 ($H_{rms,0}$) incident wave height and H_1 ($H_{rms,1}$) damped wave height behind

185   the section:

$$\frac{H_0 - H_1}{H_0} = \frac{\alpha x}{1 + \alpha x} \text{ (reg. waves)}, \qquad \frac{H_{rms,0} - H_{rms,1}}{H_{rms,0}} = \frac{\alpha x}{1 + \alpha x} \text{ (irreg. waves)}$$

186   In which

$$\alpha = A \frac{S_D}{S_S^2} C_D k \left[\frac{\sinh^3 kS_H + 3 \sinh kS_H}{\sinh kh(\sinh 2kh + 2kh)} \right]$$

187   Where

188 $A = 4/(9\pi)\, H_0$ for regular waves and $A = 2/(3\sqrt{\pi})\, H_{rms,0}$ for irregular waves, $k = 2\pi/L$ (L = wave

189 length of peak period T_p), h = water depth, S_D = stem diameter, S_S = stem spacing, S_H = stem height as

190 measured on the test section for *Elymus*, the dominant species (h = 2 m, S_D = 1.3 mm, S_S = 28.6 mm,

191 S_H = 700 mm; Table 1).

192 The drag coefficient C_D was determined as a function of the Reynolds Number Re_v[22]:

193
$$C_D = -0.046 + \left(\frac{305.5}{Re_v}\right)^{0.977} \text{ (regular waves; } r^2 = 0.97)$$

194
$$C_D = 0.159 + \left(\frac{227.3}{Re_v}\right)^{1.615} \text{ (irregular waves; } r^2 = 0.99)$$

195 With
$$Re_v = U_{max}\, \frac{S_D}{v_k}$$

196

197 Where v_k is the kinematic viscosity (1×10^{-6} m^{2}s^{-1}) and U_{max} = f(H_0 or $H_{rms,0}$ resp. and T_p) the orbital

198 velocity at the bottom in front of the vegetated section based on linear wave theory.

199 **[For further details on field site, test section construction, wave analysis and methods used to**

200 **analyse vegetation behaviour and damage as well as soil elevation change, refer to the**

201 **Supplementary Information.]**

202 **Author contributions**. IM, BvW, GW, TS, TB, SS, MK, MML, MP, and KJ designed the experiment. IM,

203 FR, MK, MML, MP, TS, GW, and SS participated in the construction and running of the experiment.

204 IM and MK conducted the wave data analysis with FR processing biomass and video information. IM

205 processed the soil elevation data and wrote the initial manuscript. All authors contributed to and

206 approved the final manuscript.

207 **References:**

208 1.   Woodruff, J. D., Irish, J. L. & Camargo, S. J. Coastal flooding by tropical cyclones and sea-level

209   rise. *Nature* **504,** 44–52 (2013).

210   2.   Wong, P.P. *et al*. in *Climate Change 2014: Impacts, Adaptation, and Vulnerability. Part A:*

211   *Global and Sectoral Aspects. Contribution of Working Group II to the Fifth Assessment Report*

212   *of the Intergovernmental Panel on Climate Change* (eds Field, C.B. *et al*.) Ch. 5 (IPCC,

213   Cambridge Univ. Press, 2014).

214   3.   Loder, N. M., Irish, J. L., Cialone, M. A. & Wamsley, T. V. Sensitivity of hurricane surge to

215   morphological parameters of coastal wetlands. *Estuar. Coast. Shelf Sci.* **84,** 625–636 (2009).

216   4.   Koch, E. W. *et al.* Non-linearity in ecosystem services: temporal and spatial variability in

217   coastal protection. *Front. Ecol. Environ.* **7,** 29–37 (2009).

218   5.   Shepard, C. C., Crain, C. M. & Beck, M. W. The protective role of coastal marshes: a

219   systematic review and meta-analysis. *PLoS One* **6,** e27374 (2011).

220   6.   Gedan, K. B., Kirwan, M. L., Wolanski, E., Barbier, E. B. & Silliman, B. R. The present and future

221   role of coastal wetland vegetation in protecting shorelines: answering recent challenges to

222   the paradigm. *Clim. Change* **106,** 7–29 (2010).

223   7.   Temmerman, S. *et al.* Ecosystem-based coastal defence in the face of global change. *Nature*

224   **504,** 79–83 (2013).

225   8.   Bouma, T. J. *et al.* Identifying knowledge gaps hampering application of intertidal habitats in

226   coastal protection: Opportunities & steps to take. *Coast. Eng.* **87**, 147–157 (2014).

227   9.   Kirwan, M. L. & Megonigal, J. P. Tidal wetland stability in the face of human impacts and sea-

228   level rise. *Nature* **504,** 53–60 (2013).

229   10.   Jones, H. P., Hole, D. G. & Zavaleta, E. S. Harnessing nature to help people adapt to climate

230   change. *Nat. Clim. Chang.* **2,** 504–509 (2012).

231   11.   Kabat, P. *et al.* Dutch coasts in transition. *Nat. Geosci.* **2,** 450–452 (2009).

232   12.   Barbier, E. B. *et al.* The value of estuarine and coastal ecosystem services. *Ecol. Monogr.* **81,**

233   169–193 (2011).

234   13.   US Army Corps of Engineers, Coastal Risk Reduction and Resilience (USACE, 2013);

235   http://www.corpsclimate.us/docs/USACE_Coastal_Risk_Reduction_final_CWTS_2013-3.pdf

236   14.   Spalding, M.D. *et al*. Coastal ecosystems: a critical element of risk reduction. *Conserv. Lett.* **7**,

237   293-301 (2014).

238   15.   Fagherazzi, S., Carniello, L., D'Alpaos, L. & Defina, A. Critical bifurcation of shallow microtidal

239   landforms in tidal flats and salt marshes. *Proc. Natl. Acad. Sci. U. S. A.* **103,** 8337–8341 (2006).

240   16.   Mariotti, G. & Fagherazzi, S. Critical width of tidal flats triggers marsh collapse in the absence

241   of sea-level rise. *Proc. Natl. Acad. Sci. U. S. A.* **110,** 5353–5356 (2013).

242   17.   Möller, I., Spencer, T., French, J. R., Leggett, D. J. & Dixon, M. Wave transformation over salt

243   marshes: A field and numerical modelling study from North Norfolk, England. *Estuar. Coast.*

244   *Shelf Sci.* **49,** 411–426 (1999).

245   18.   Yang, S. L., Shi, B. W., Bouma, T. J., Ysebaert, T. & Luo, X. X. Wave attenuation at a salt marsh

246   margin: A case study of an exposed coast on the Yangtze Estuary. *Estuaries and Coasts* **35,**

247   169–182 (2011).

248   19.   Möller, I. & Spencer, T. Wave dissipation over macro-tidal saltmarshes : Effects of marsh edge

249   typology and vegetation change. *J. Coast. Res.* **36,** 506–521 (2002).

250   20.   Duarte, C. M., Losada, I. J., Hendriks, I. E., Mazarrasa, I. & Marbà, N. The role of coastal plant

251   communities for climate change mitigation and adaptation. *Nat. Clim. Chang.* **3,** 961–968

252   (2013).

253   21.   Feagin, R. A. *et al.* Does vegetation prevent wave erosion of salt marsh edges? *Proc. Natl.*

254   *Acad. Sci. U. S. A.* **106,** 10109–10113 (2009).

255   22.   Paul, M. & Amos, C. L. Spatial and seasonal variation in wave attenuation over *Zostera noltii*.

256   *J. Geophys. Res*. **116**, C08019 (2011).

257   23.   Mendez, F., Losada, I., & Losada, M. Hydrodynamics induced by wind waves in a vegetation

258   field. *J. Geophys. Res*. **104, C8**, 18383-18396 (1999).

259   24.   Kobayashi, N., Raichle, A., & Asano, T. Wave attenuation by vegetation. *J. Waterw. Port*

260   *Coast. Ocean Eng.*, **119**, 30-48 (1993).

261   25.   Mullarney, J. C. & Henderson, S. M. Wave-forced motion of submerged single-stem

262   vegetation. *J. Geophys. Res.* **115,** C12061 (2010).

263   26.   Howes, N. C. *et al.* Hurricane-induced failure of low salinity wetlands. *Proc. Natl. Acad. Sci.*

264   *U.S.A.* **107,** 14014–14019 (2010).

265   27.   Allen, J. R. L. Morphodynamics of Holocene salt marshes: A review sketch from the Atlantic

266   and Southern North Sea coasts of Europe. *Quat. Sci. Rev.* **19**, 1155-1231 (2000).

267   28.   Fagherazzi, S., Mariotti, G., Wiberg, P. L. & McGlathery, K. J. Marsh collapse does not require

268   sea level rise. *Oceanography* **26,** 70–77 (2013).

269   29.   Dalrymple, R. A., Kirby, J. T. & Hwang, P. A. Wave diffraction due to areas of energy

270   dissipation. *J. Waterw. Port Coast. Ocean Eng*. **110** (1), 67-79 (1984).
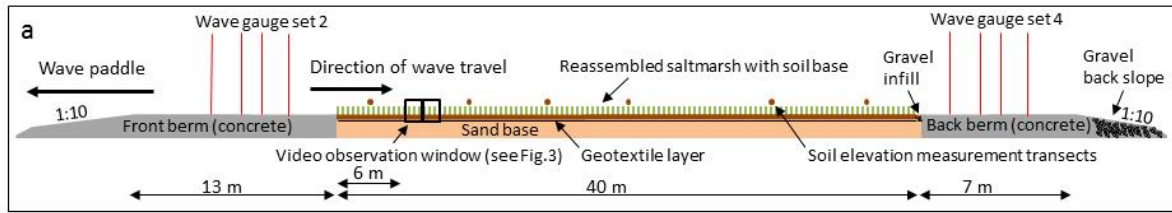
271 30. Mendez, F. & Losada, I. An empirical model to estimate the propagation of random breaking

272   and nonbreaking waves over vegetation fields. *Coast. Eng*. **51**(2), 103-119 (2004).

273

274 Correspondence and requests for materials should be addressed to Iris Möller at

275 im10003@cam.ac.uk.

283

284

Figure 1 | Experimental set-up and photographs of excavation. a, General experimental set-up in the wave flume, with position of recording equipment relevant to reported results. **b,** Excavation of marsh blocks, northern German Wadden Sea (53°42.754 N, 07°52.963 E). **c,** Marsh blocks with *Elymus* vegetation cover prior to positioning in the flume test section. **d,** Reassembled salt marsh inside the 5-m-wide flume, looking towards the wave generator; lamps are mounted at about 3m above the soil surface.

291
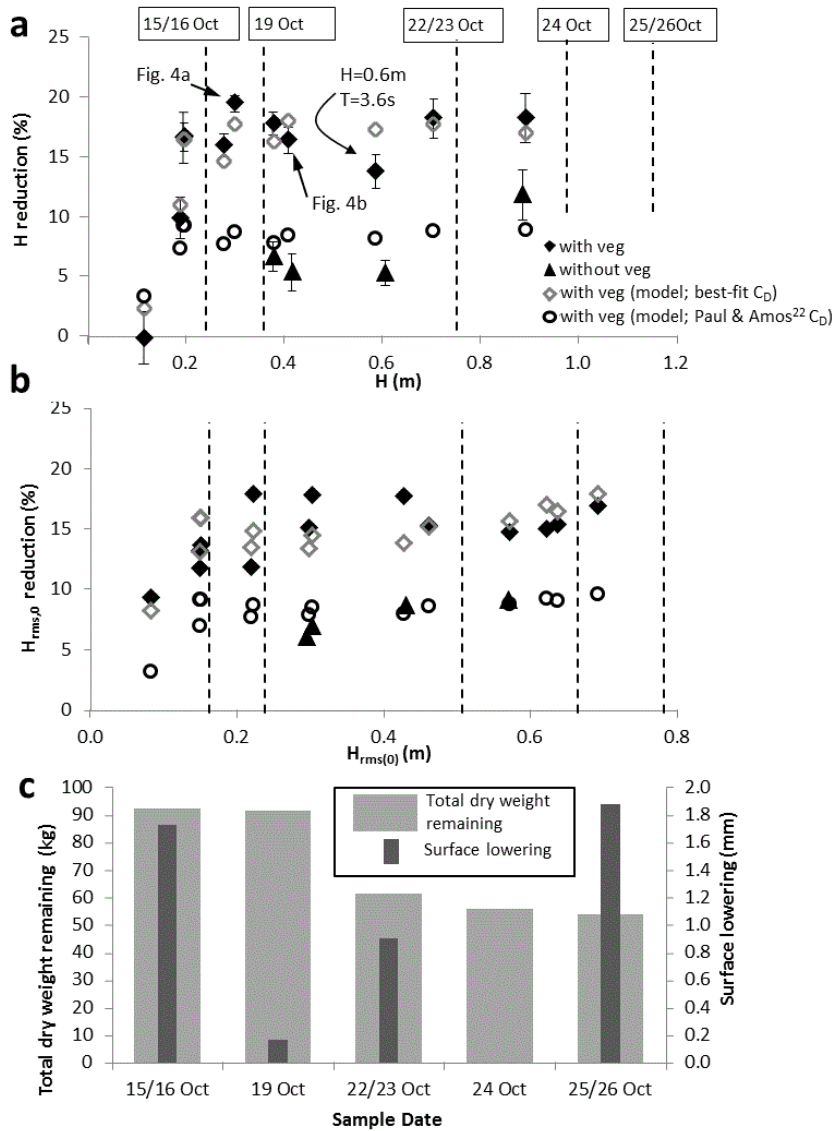
Figure 2 | Wave dissipation across 40 m of vegetated and mowed salt marsh. a,b Percentage reduction for regular waves (**a**: H) and irregular waves (**b**: $H_{rms,0}$), error bars in **a** refer to the mean ± 1 SD; filled diamonds/triangles refer to observed vegetated/mowed conditions, open diamonds and circles refer to modelled vegetated conditions using best-fit and ref.[22] C_D values respectively, vertical lines mark times of soil elevation and floating debris measurement (Fig. 2c) **c,** Plant biomass (light thick bars) remaining and mean surface elevation lowering (dark thin bars; standard error of ±10.4mm not shown).

299
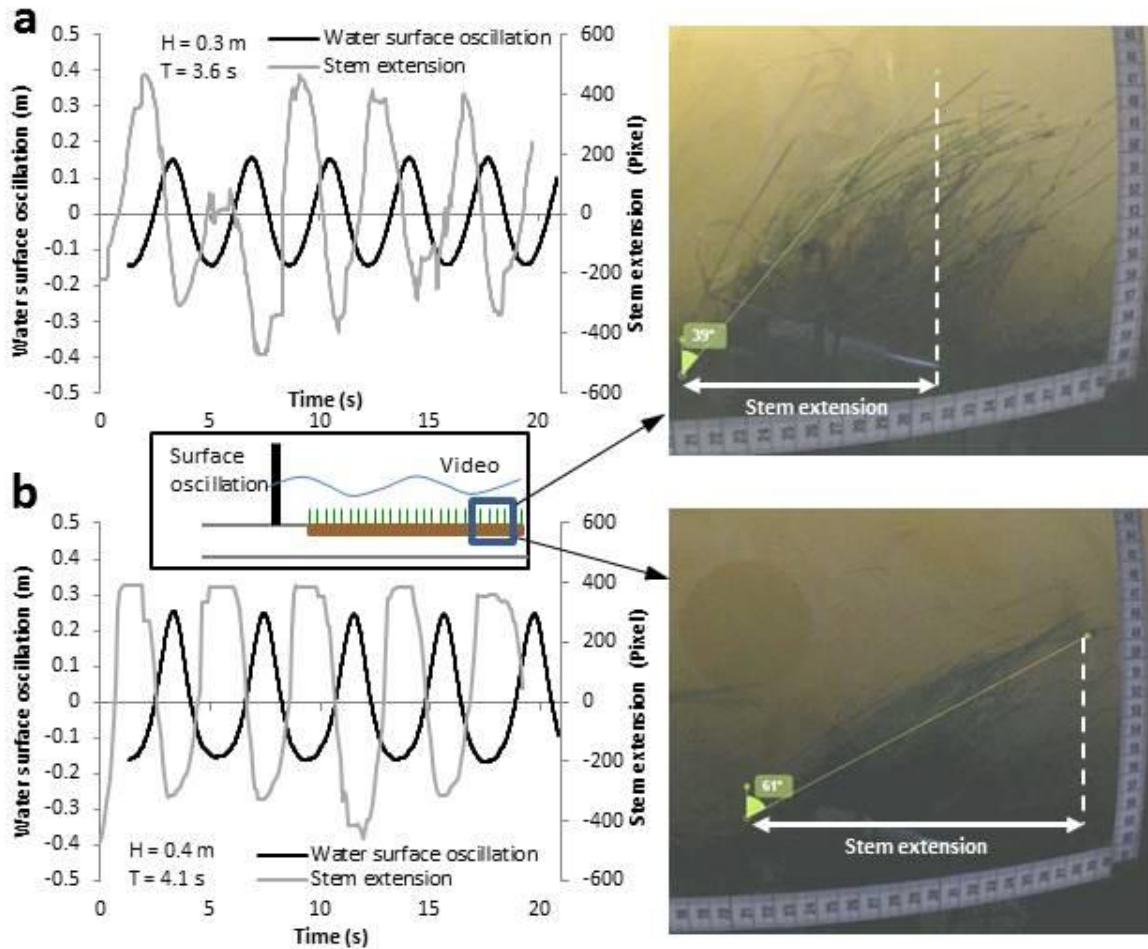
Figure 3 | *Puccinellia* **plant canopy movement during wave motion. a,b** Water level excursion (y-axis) and time-trace of horizontal stem extension (video pixel units; positive values in the direction of wave motion (white arrow in photographs)) under waves experiencing maximum dissipation (Fig. 2a) (**a**) and waves of greater height and period but experiencing lower dissipation (Fig. 2a) (**b**). A phase shift results from water level measurement occurring approximately 10m forward of video observations (see also experimental set-up in Fig. 1a). Lack of visibility in highly turbid water precluded analysis of conditions at H=0.6m, T=3.6s (Fig. 2a).

307

16

308　**Table 1 | Plant stem flexibility (Young's Modulus), height, density, and diameter and soil bulk**

309　**density at the field site where marsh blocks were extracted and in the flume immediately before**

310　**the experimental runs (means ± one s.d.).**

|	Stem flexibility Young's bending modulus (MPa)		Stem height [mm]	Stem diameter [mm]		Stem density (number per 20 x 20 cm quadrat)		Dry soil bulk density (g cm^{-3})	
	Mean	N	Mean	Mean	N	Mean	N	Mean	N
Puccinellia (Flume)	111.6 ± 66.3	17	220 ± 30	1.1 ± 0.3	17	-	-	0.6 ± 0.3	10
Puccinellia (Field)	284.5 ± 369.1	17	-	1.2 ± 0.2	17	-	-	0.7 ± 0.5	20
Elymus (Flume)	2,696.3 ± 1,963.8	18	700 ± 10	1.3 ± 0.3	18	49 ± 23	10	0.7 ± 1.0	20
Elymus (Field)	2,514.6 ± 2,977.1	18	-	1.7 ± 0.4	18	68 ± 8	10	0.8 ± 0.7	20

311

312

Wave attenuation over coastal salt marshes under storm surge conditions

314

315 Iris Möller, Matthias Kudella, Franziska Rupprecht, Tom Spencer, Maike Paul, Bregje K. van

316 Wesenbeeck, Guido Wolters, Kai Jensen, Tjeerd J. Bouma, Martin Miranda-Lange

317

318 **SUPPLEMENTARY FIGURE, TABLE, AND METHODS**
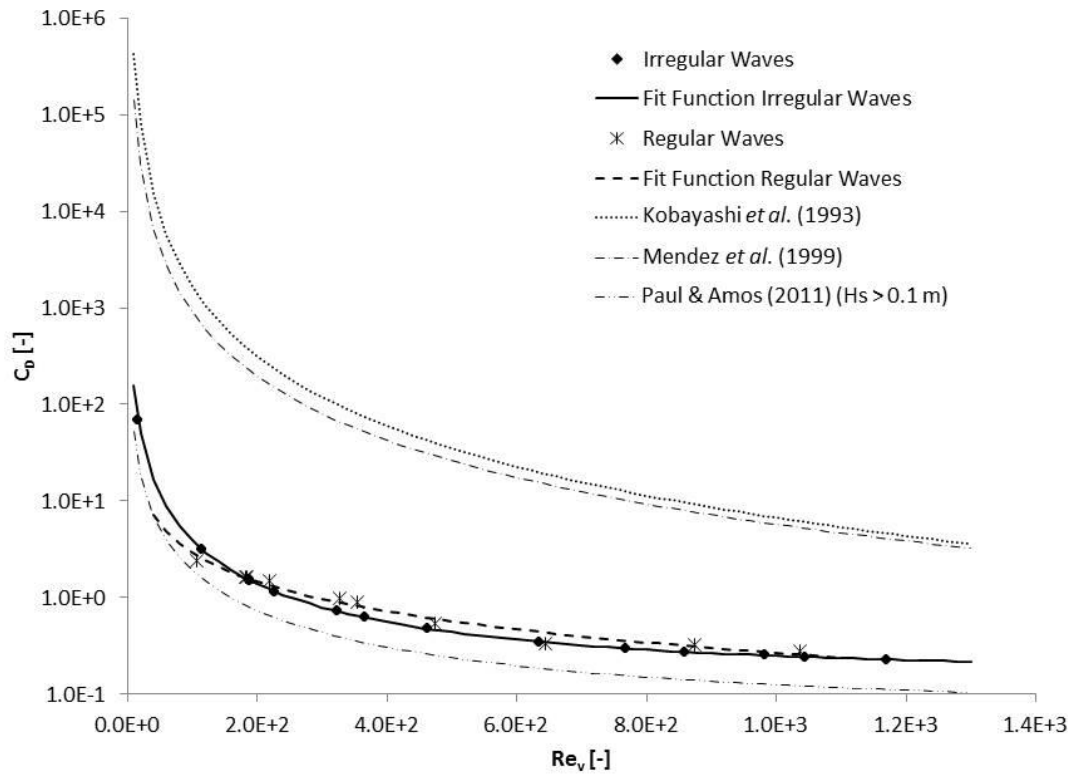
319

320 **Figure 4 | Relationship between C_D and vegetation Reynolds number Re_V and best fit for regular**

321 **and irregular waves.** Also shown are the best fit lines of Kobayashi et al.[24], Mendez et al.[23], and Paul

322 and Amos[22]. For best fit line equation and coefficients, see methods and Table 2.

323

324 **Table 2 | Coefficients of the exponential decay function relating C_D to Re_V as determined in**

325 **previous studies and this experiment.**

Study	Vegetation type	a	b	c
Kobayashi et al. (1993)[24] (data from Asano et al. (1988))	Kelp	0.08	2200	2.40
Mendez et al. (1999)[23]	Kelp (rigid)	0.08	2200	2.20
	Kelp (swaying)	0.40	4600	2.90
Paul and Amos (2011)[22]	Seagrass	0.06	153	1.45
This experiment	Salt marsh (regular waves)	-0.05	306	0.98
	Salt marsh (irregular waves)	0.16	227	1.62

SUPPLEMENTARY METHODS

Field site. The vegetated marsh blocks were cut from a natural marsh on the mainland coast in Eastern Frisia, German Wadden Sea (53°42.754 N; 07°52.963 E) in June 2012. Blocks were lifted mechanically and placed on a wooden pallet, lined with a plastic sheet covered by a layer of geotextile. The experiment could not be scheduled prior to autumn 2013 and marsh blocks were stored outdoors in appropriate temperature/moisture conditions and with fences to control for herbivory for 14 months. For marsh construction in the flume, individual blocks were separated from their wooden base, lowered into position and keyed to neighbouring blocks using a marsh clay sealant.

Experimental test section illumination. Illumination of plants on the test section was achieved by 60 flume wall-mounted lamps (GE 750W 400V PSL or equivalent).

Wave analysis. For irregular wave tests, time-series of water level fluctuations were used to determine incident and reflected waves using the standard three-gauge method of Mansard and Funke[31]. After applying a low pass filter at $3.3f_p$ (with f_p = peak frequency) and a high pass filter at $f_p/2.1$, incident spectra were used to compute the peak wave period (T_p). After a reverse FFT of the incident spectrum the root-mean-square wave height in front of ($H_{rms,0}$) and behind ($H_{rms,1}$) the vegetated section was calculated according to $H_{rms} = \sqrt{\frac{1}{N}\sum_{i=1}^{N} H_i^2}$, where N is the number of incident waves and H_i the individual waves in the time series of incident waves.

Vegetation behaviour and damage. The Youngs' Modulus was measured according to the method described in Miler *et al.*[32]. Bending tests were performed with a ZWICK 1120 mechanical testing machine using a 100 N load cell (resolution 0.012 N) and a 1000 N load cell (resolution 0.12 N); Zwick GmbH & Co. KG, Ulm, Germany). Videography from behind lateral observation windows was used to record plant movement at a frequency of 10 Hz (Fig. 1a). Movement of plant stems was analysed

350   using frame-by-frame tracking of stems[23], using 'Kinovea' video analysis software. All floating organic

351   debris was removed using a net (1 cm mesh size) when necessary and total dry weight was

352   determined.

353   **Soil elevation measurements.** Soil elevation was measured from an access platform, lowered into

354   six cross-flume positions, whenever the vegetated section was drained (Fig. 1a). The surface of the

355   platform was approximately 30 cm above the soil base and temporarily locked into fixed basal slots,

356   to within 1 mm accuracy. Soil surface elevations were determined with respect to a horizontal bar

357   fixed to the platform. Pins were lowered vertically onto the soil surface every 20 cm along the bar to

358   determine soil surface elevation to millimetre accuracy.

359   31.   Mansard, E. P. D. & Funke, E. R. The measurement of incident and reflected spectra using a

360   least squares method. *Proc. 17th Coast. Eng. Conf. Vol 1* 154–172 (American Society of Civil

361   Engineers, 1980).

362   32.   Miler, O., Albayrak, I., Nikora, V. & O'Hare, M. Biomechanical properties of aquatic plants and

363   their effects on plant-flow interactions in streams and rivers. Aquat. Sci. **74**, 31-44